Osseointegration of porous apatite-wollastonite and poly(lactic acid) composite structures created using 3D printing techniques

Authors:

Ion Tcacencu[1], Natacha Rodrigues[2], Naif Alharbi[2], Matthew Benning[2], Sotiria Toumpaniari[2], Elena Mancuso[2], Martyn Marshall[3], Oana Bretcanu[2], Mark Birch[4], Andrew McCaskie[4], Kenneth Dalgarno[2, *]

[1] Department of Dental Medicine, Karolinska Institutet, Box 4064, 14104 Huddinge, Sweden.

[2] School of Mechanical and Systems Engineering, Newcastle University, Newcastle upon Tyne, NE3 1PS, UK.

[3] Glass Technology Services Ltd, 9 Churchill Way, Sheffield, S35 2PY, UK.

[4] Department of Surgery, Cambridge University, Addenbrooke's Hospital, Hills Road, Cambridge, CB2 0QQ, UK.

* corresponding author

Abstract

A novel apatite-wollastonite/poly(lactic acid) (AW/PLA) composite structure, which matches cortical and cancellous bone properties has been produced and evaluated in vitro and in vivo. The composites structure has been produced using an innovative combination of 3D printed polymer and ceramic macrostructures, thermally bonded to create a hybrid composite structure. In vitro cell assays demonstrated that the AW structure alone, PLA structure alone, and AW/PLA composite were all biocompatible, with the AW structure supporting the proliferation and osteogenic differentiation of rat bone marrow stromal cells. Within a rat calvarial defect model the AW material showed excellent osseointegration with the formation of new bone, and vascularisation of the porous AW structure, both when the AW was implanted alone and when it was part of the AW/PLA composite structure. However, the AW/PLA structure showed the largest amount of the newly formed bone in vivo, an effect which is considered to be a result of the presence of the osteoinductive AW structure stimulating bone growth in the larger pores of the adjacent PLA structure. The layered AW/PLA structure showed no signs of delamination in any of the in vitro or in vivo studies, a result which is attributed to good initial bonding between polymer and ceramic, slow resorption rates of the two materials, and excellent osseointegration. It is concluded that macro-scale composites offer an alternative route to the fabrication of bioactive bone implants which can provide a match to both cortical and cancellous bone properties over millimetre length scales.

1. Introduction

The varying mechanical properties of bone throughout its volume means that it is difficult for a synthetic implant formed from a single material to match the anisotropic properties in different regions. Furthermore, discrete anatomical regions such as cortical, sub-chondral and cancellous bone each have their own unique mechanical properties and architectures (Keaveny and Hayes, 1993; Li and Aspden, 1997). Ceramic-polymer composites have been proposed as bone implants most commonly as particulate reinforced polymer structures (Rezwan et al., 2006), either solid or porous. This produces a material which has the strength of the polymer phase, and a slightly higher modulus than the polymer phase, which for most resorbable biopolymers is normally a good match to the mechanical properties of cancellous bone (Rezwan et al., 2006). The mechanical response of an implant can also be varied through design of the structure and in recent years various additive manufacturing techniques have been used, along with other techniques, to create macro-porous structures in metals, polymer and ceramic materials (Mota et al., 2015; Wang et al., 2016), again potentially allowing properties to be matched to different regions of bone. However, the wide range of variation in properties of natural bone is such that they may be better reproduced by bringing together two distinct structures made from two different biomaterials.

The aim of the study reported here was to evaluate the potential for porous ceramic-polymer composites in bone implants, with the different constituent parts of the composite engineered to have properties which equate to both cortical and cancellous bone. The two phases of the composite were a macroporous poly(lactic acid) (PLA) structure, with mechanical properties which match those of cancellous bone (Rodrigues et al., 2016), together with microporous apatite-wollastonite glass-ceramic (AW), with mechanical properties which approach those of cortical bone (Mancuso et al., 2017). PLA and AW are both recognised biomaterials (Narayanan et al., 2016; Kokubo, 1991), with established methods for processing them to create porous structures. The overall approach adopted was to create the individual structures and a macro-scale composite which combined the two structures,

and to evaluate these in vitro and in vivo to determine the value that the approach might offer in terms of the design of structural composite implants.

2. Materials and Methods

2.1 Raw Materials

AW frit and powders were produced to a formulation originally proposed by Kokubo (1991): weight% 4.6 MgO, 44.7 CaO, 34 SiO_2, 16.2 P_2O_5 and 0.5 CaF_2. Maltodextrin (MD) powder (99.5% purity) was purchased from Oneon (Bristol, UK). The AW and maltodextrin powders were separately ground and sieved, and then mixed to create a powder blend which was 55 wt% AW powder with particle sizes in the 54-90 μm range, 15 wt% AW powder with particle sizes in the 0-53 μm range, and 30% MD powder with particle sizes in the 0-53 μm range. A 3 mm nominal diameter PLA filament (4032D, Nature Works®) with an L-lactide: D-lactide ratio of 98:2 and a density of 1.24 g/cm^3 was the material used to create the porous polymer structure.

2.2 Indirect 3D Printing of AW

The indirect 3D printing processing route was to use a ZPrinter 310 Plus 3D printer (ZCorp, USA) to produce a green part, which was then sintered in a furnace (Carbolite, Germany). The manufacturing process is described in Mancuso et al. (2016). In brief, to produce the green part the AW/MD powder blend was loaded into the printer, and the zb®60 clear binder (ZCorp) jetted to sequentially bind together layers of powder. The ZPrinter machine settings were: layer thickness 0.1 mm; bleed compensation off; shell saturation level 100%; shell binder/volume ratio 0.215; core saturation level 100%; and core binder/volume ratio 0.107. The green parts created were disks of nominal diameter of 10.25 mm, and nominal heights of 1.13 or 2.25 mm. The green parts were sintered according to a sintering cycle originally developed by Xiao et al. (2008). From room temperature the temperature was raised at 10ºC/min to 779ºC, the temperature was then held at 779ºC for 1 hour before the

temperature was raised to 1150ºC at 10ºC/min, where the temperature was held constant for 1 h, after which the disks were cooled to room temperature at the natural rate of the furnace. AW disks were sterilised in a steam autoclave at 121ºC for 15 mins.

2.3 Fused Filament Fabrication of PLA Structures

For the PLA structure fabrication a 2-step manufacturing route described by Rodrigues et al. (2016) was used. Briefly the first step consisted of printing PLA rectangular porous bars with a nominal length or 184 mm, nominal width of 29 mm, and nominal heights of 1 or 2 mm, using a Fused Filament Fabrication (FFF) machine (Ultimaker 2). Then porous discs with nominal diameters of 10 mm were laser cut (LS6090, HPC Laser LTD) from the printed bars, using laser velocity and power of 25 mm/sec and 20 Watts respectively. The PLA structures were sterilised through exposure to 2.5 MRad gamma irradiation.

2.4 Thermal Bonding of AW and PLA Composite Structures

The composite structures consisted of a PLA porous disk 8 mm diameter and 1 mm thick thermally mounted to the surface of a AW disk, of the same diameter, and also 1 mm thick. The thermal bonding process consisted of preheating, bonding and quenching phases. The AW disks were placed on a standard laboratory hot plate set to 250ºC. After a preheating phase of 120 seconds a PLA disk was then positioned, as to be concentric, on the top surface of the AW disk. The PLA was allowed to thermally adhere to the surface of the AW for 5-8 seconds before being quenched in pure ethanol. The composite structures were then set aside to allow any ethanol remaining after quenching to evaporate. The composite structures were also sterilised through exposure to 2.5 MRad gamma irradiation.

2.5 Material and Structural Characterisation Techniques

An Olympus micropublisher 5.0 RTV digital microscope, an SEM Philips XL30 ESEM-FEG and an Xradia VersaXRM-410 micro-CT were used to image samples. X-ray powder diffraction spectra were obtained from a PANalytical X'Pert Pro Multipurpose Diffractometer.

Dimensional measurements were made using Mitutoyu digital calipers. Total and open porosity levels in the AW disks were determined through weighing samples of known dimensions using a digital scale (KERN ABT 220-5DM) when dry, wet and submerged and applying Archimedes principle. Porosity levels in the PLA structures were determined through weighing samples of known external dimensions and using the density of PLA to infer the ratio of PLA to pores.

2.6 In Vitro Assays

Bone marrow-derived stromal cells (BMSCs) were isolated from adult male Sprague–Dawley rats as described by Tour et al. (2014), and used at passages 3 to 5. For all the in vitro assays, the BMSCs were seeded in triplicate for each material into 48-well plates (Corning) on the top of the sample discs (10,000 cells/disc/0.5 ml culture media/well) in a humidified atmosphere of 5% CO_2 at 37°C. The experiments were repeated twice.

2.6.1 Cytocompatibility

The cytocompatibility was assessed by 3-(4,5-dimethythiazol-2-yl)-2,5-diphenyl tetrazolium bromide colorimetric assay (Cell Proliferation Kit I (MTT), Roche Diagnostics) or by lactate dehydrogenase (LDH) activity assay (CytoTox 96® Non-Radioactive Cytotoxicity Assay kit, Promega Co.) according to manufacturer's instructions after 24h or 48h direct contact culture in alpha-minimum essential medium supplemented with 10% foetal bovine serum and antibiotics/antimycotics (all from Life Technologies, Inc.).

2.6.2 Osteogenic differentiation

Alkaline phosphatase (ALP) activity was used as a marker for the osteogenic differentiation of the BMSCs in the presence of the disc samples. For the ALP assay, the normal medium was replaced with commercially available osteogenic medium (Osteogenic Differentiation BulletKit™, Lonza) containing ascorbic acid, beta-glycerophosphate, and dexamethasone. After 7 and 14 days of the direct contact osteogenic culture, the BMSCs were washed with phosphate buffer, then lysed with 0.2% Triton X-100 (Sigma-Aldrich), and sonicated. The ALP activity was quantified by measuring the rate of formation of p-nitrophenol (pNP) produced by

hydrolysis of p-nitrophenylphosphate (Sigma-Aldrich) in 1M diethanolamine solution, buffered to pH 9.8 at 37°C for 30 min using a UV/Vis spectrometer, measuring at 405 nm (Labsystems Multiskan MS). The ALP activity was normalized to the cell number correlated to LDH values, as reported previously by Allen et al. (1994), using the CytoTox 96® Non-Radioactive Cytotoxicity Assay kit, Promega Co. according to the manufacturer's instructions. The final ALP data were expressed as μM pNP/1000 cells. The BMSCs cultured alone on tissue culture plastic were used as controls.

2.7 In Vivo Study

The experiments were approved by the Stockholm South Ethical Committee in accordance with the policy on human care and use of laboratory animals.

2.7.1 In Vivo Model

Fifteen adult Sprague–Dawley male rats (~350 g) were used. The rats were kept under uniform conditions for a period of least one week before commencement of the experiment. Free access to water and standard pelleted food was provided throughout the experiment. The rats were randomly divided into three groups based on the biomaterials they received: PLA discs (n=3), AW discs (n=6), and AW/PLA discs (n=6). Before implantation, the discs were washed with saline solution. A critical-size calvarial defect model was used (Tour et al., 2014). The rats were anaesthetized by subcutaneous injection of Ketamine (Ketaminol, Intervet AB) with Xylazine (Rompun, Bayer HealthCare). During the surgery the rat was maintained on a heating pad. The rat's head was shaved, washed with 70% ethanol solution, and afterwards an incision was made in the sagittal plane across the cranium. The skin and underlying tissues including the periosteum and temporal muscle were detached to expose the calvarial bone. An 8-mm full thickness circular defect was created on the left parietal region using a trephine drill with a sterile saline irrigation. The disc was placed into the bone defect. The incisions were closed with single sutures in two layers.

2.7.2 Tissue preparation, histology and histomorphometric analysis

The rats were euthanized by CO_2 inhalation at 12 weeks after surgery. The calvarial bone was surgically retrieved, and histologically processed. The samples were fixed in 4% neutral-buffered formaldehyde overnight then decalcified in 12.5% ethylenediaminetetraacetic acid, and embedded in paraffin; 5-µm serial sections were prepared parallel to the sagittal line and stained with Haematoxylin and Eosin for the assessment of the general morphology or Wright-Giemsa for the assessment of local cellular inflammatory reaction. Two central sections from calvaria bone defects treated with AW or AW/PLA were assessed histomorphometrically using an image-analysis software (ImageJ, National Institutes of Health, USA) and the percentage of new bone formation was quantified. The data were statistically analyzed using the Mann-Whitney U-test, and significance was defined as $p<0.05$.

3. Results

3.1 Characterisation of AW, PLA, and AW/PLA Structures

For the sintered AW disks (Figure 1) the total porosity was measured to be 41.85% (standard error (s.e.), 0.94%, n=10), with 12.4% (s.e. 0.29%, n=10) of this open porosity. The sintered disks were approximately 8 mm diameter and 2 mm thickness. The PLA "logpile" structures (Figure 2) were 60% porous. Viewed along the cylindrical axis the structure had 0.62 mm (+/- 0.02) wide PLA struts, with regular gaps of 0.55 mm (+/- 0.02) between the struts. Images of the composite structures (Figure 3) show that the height of the struts in the PLA logpiles was approximately 0.5 mm, and that porosity round the circumference of the logpile structures was open. The bonding method allowed the PLA to infiltrate into the surface of the AW plug.

The XRD spectra for the sintered AW material indicated the presence of wollastonite and calcium magnesium silicate phases, together with hydroxylapatite, calcium magnesium phosphate and fluorapatite (Figure 4).

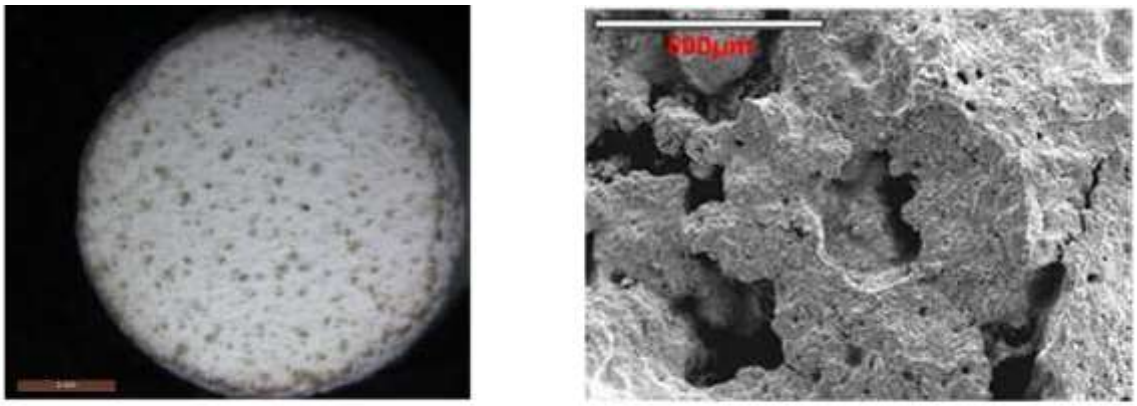

Figure 1. Sintered AW Part Morphology (a) Stereomicroscope image of top surface of sintered disk (dia. 8 mm); and (b) SEM of fracture surface showing internal structure.

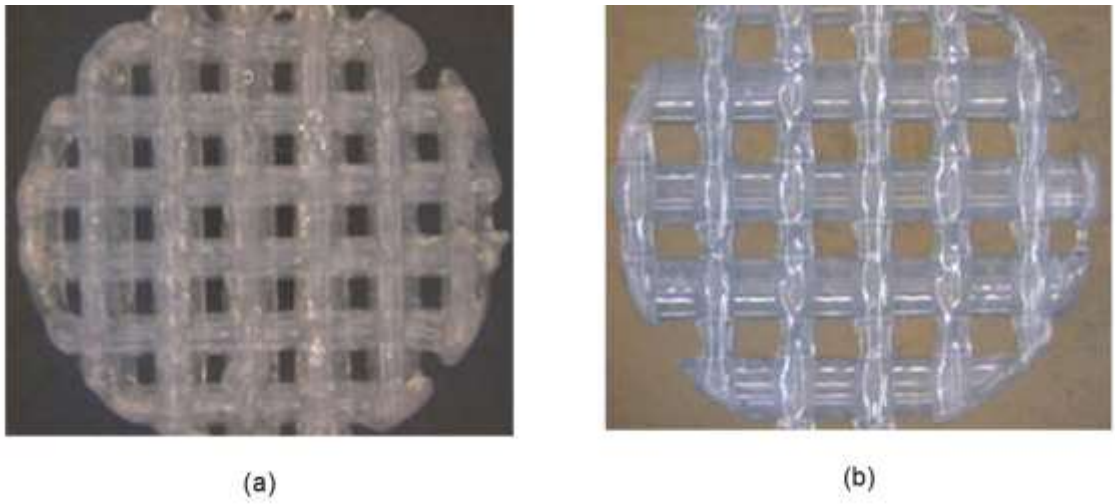

Figure 2. Stereomicroscope view of top of 8 mm diameter laser cut PLA plugs (a) 2 mm high, and (b) 1 mm high

Figure 3. Images of bonded PLA/AW composite disks: (a) & (b) stereomicroscope images of 8 mm diameter composite disk, (c) SEM image of interface.

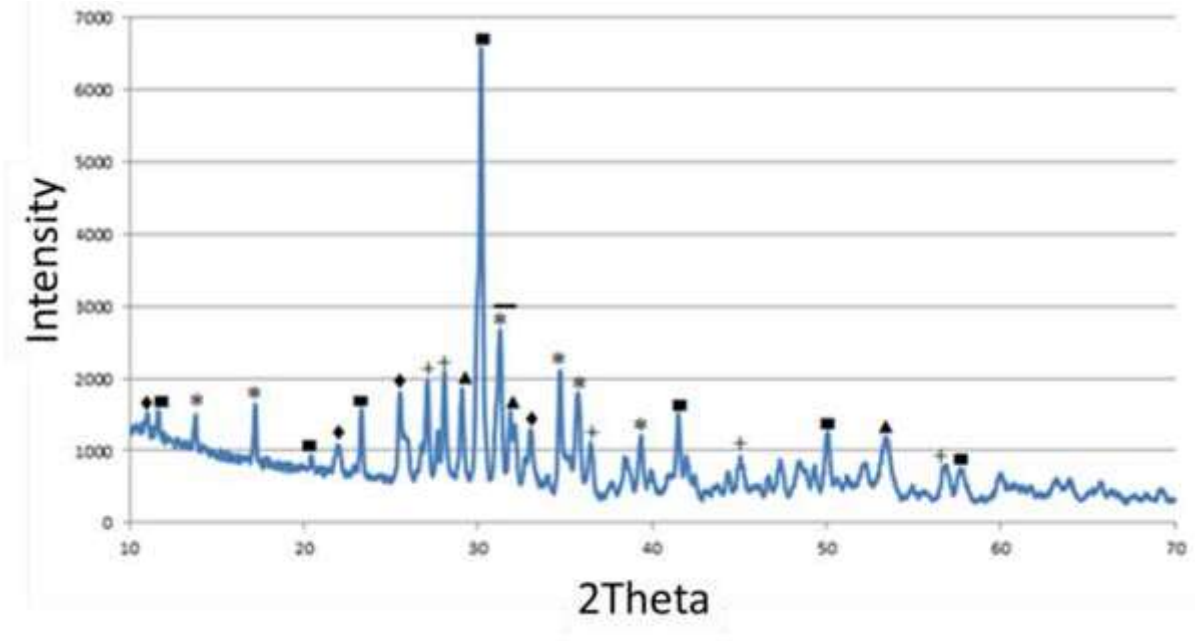

Figure 4. XRD Spectrum of Sintered Material. Phase identification: ■ wollastonite (Ref code 01-071-0880); + calcium magnesium silicate (01-076-0525); hydroxyapatite (01-073-1731); * calcium magnesium phosphate (01-087-1582); ▲ fluorapatite (01-071-0880).

3.2 In Vitro Assessment

The AW, PLA and AW/PLA discs were cyto-compatible after 24h and 48h in culture (Figure 5a). After both 7 and 14 days of osteogenic induction BMSCs had highest ALP activity when seeded directly onto the AW discs compared to the PLA or AW/PLA (Figure 5b).

3.3 In Vivo Assessment

Histological assessment of the calvarial defects demonstrated that all three types of the scaffolds were biocompatible, being well integrated into the host tissues with minimal evidence of the presence of inflammatory cells (Figure 6 (a)-(c)). For all three scaffold types the bulk of the implanted material was still present after 12 weeks.

The AW/PLA implant resulted in the largest amount of the newly formed bone, in both the AW and PLA sides of the scaffolds (Figure 6 (e)). The newly formed bone, fibrous connective

tissue and blood vessels were observed to penetrate into the AW structure (Figure 6 (d)). No new bone formation was observed in the calvaria defects treated with the PLA alone.

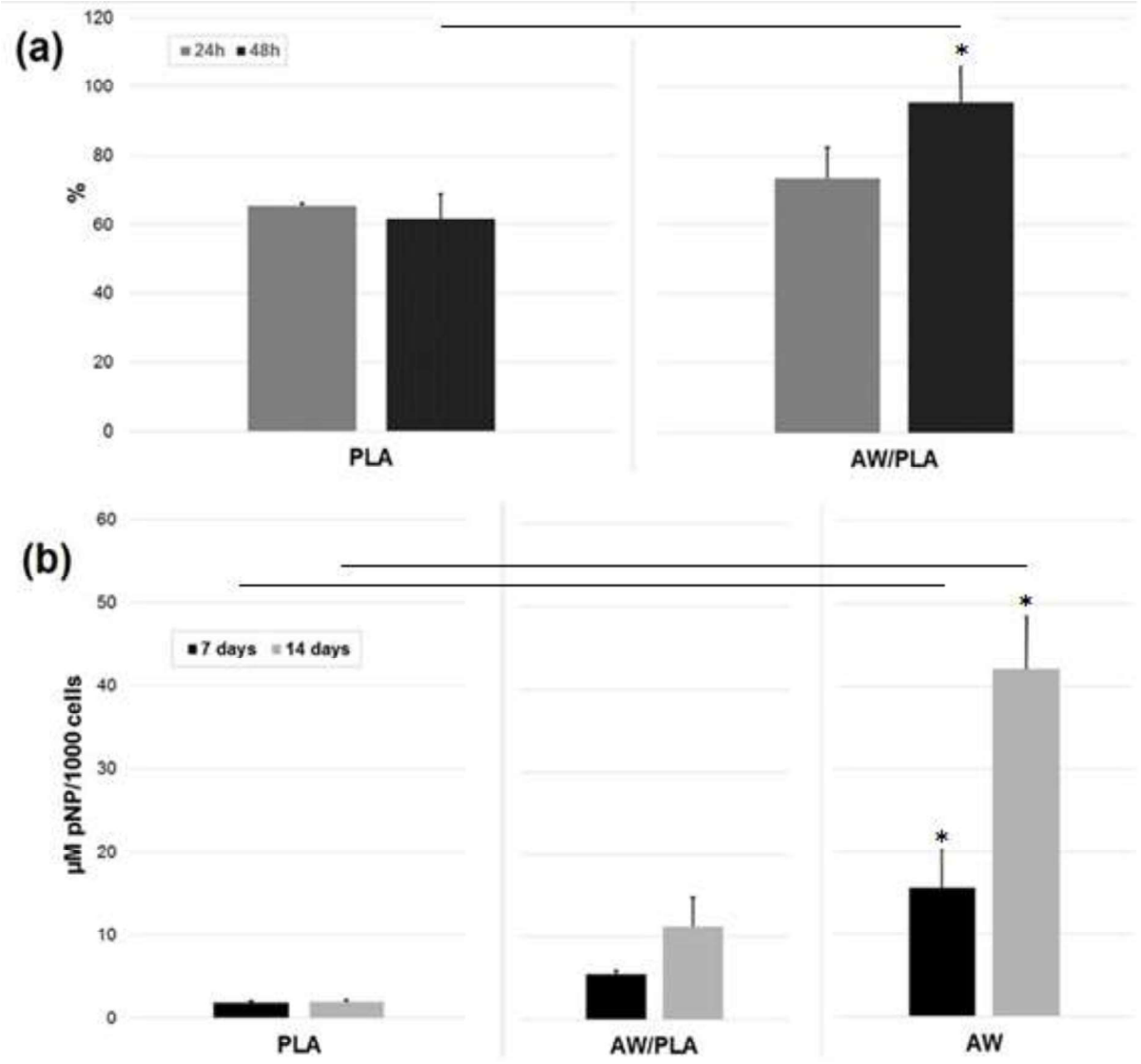

Figure 5. In vitro rat BMSCs viability data (as % vs. seeded onto AW alone ± SD) after 24h and 48h culture (a), and ALP activity data (average ± SD; µM pNP/1000 cells) after 7 days and 14 days culture (b); * $P<0.05$.

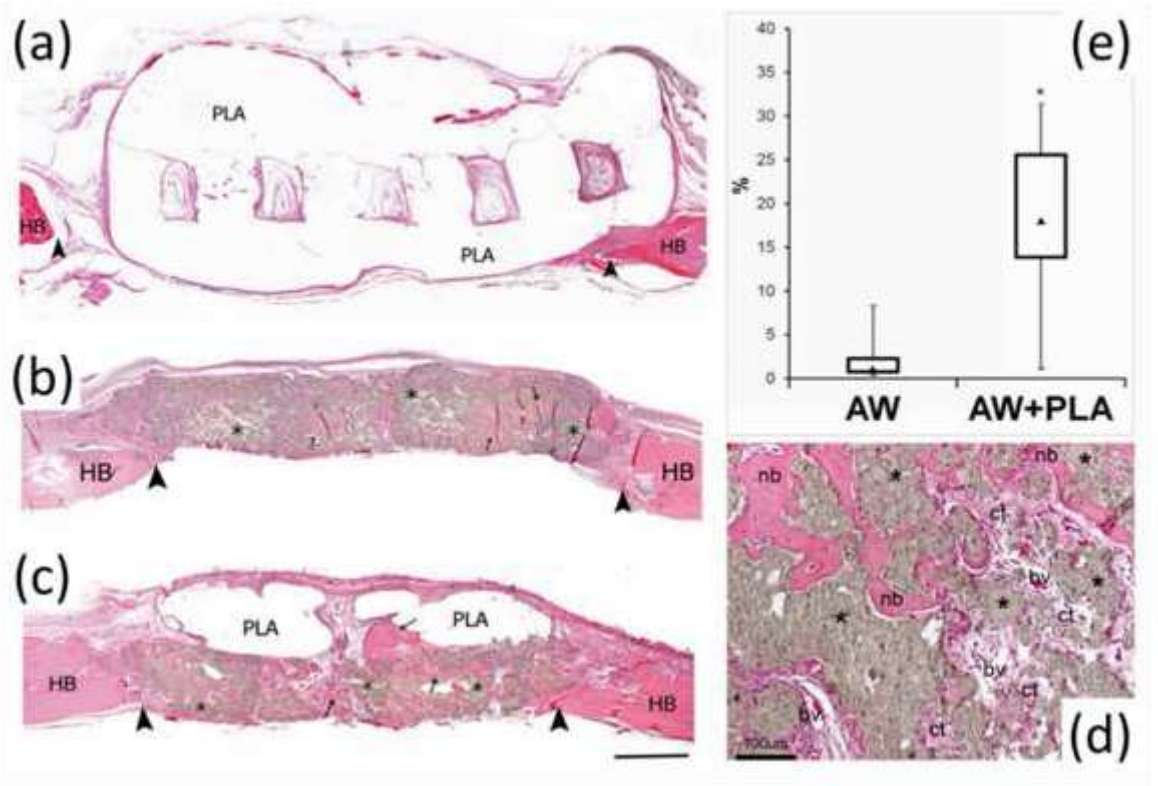

Figure 6. Histological images stained with Haematoxylin and Eosin, illustrating the general morphological aspect of the calvarial defect repair. (a) – PLA alone; (b) – AW alone; (c) – AW/PLA; Scale bar = 1 mm; HB – host bone; defect margins indicated by arrow heads; * – residual AW; (d) – representative image of enlarged area of the AW; nb – new bone; bv – blood vessel; ct – connective tissue; Scale bar = 100 μm; (e) Box plots (maximum, third quartile, median, first quartile, minimum; * *P<0.05*) representing the percentage of the newly formed bone in the calvaria defects treated with AW or AW+PLA discs.

4. Discussion

4.1 Properties and Structure

The structures achieved through FFF of PLA and binder jetting/sintering of AW were comparable in terms of porosity and morphology to those which have been previously reported (Rodrigues et al, 2016; Mancuso et al, 2017). The novel porous-porous composite structure created by thermally bonding the two structures together offers a unique

combination of mechanical properties and porosity, going beyond the range of combinations that could be achieved from a single composite material. The thermal bonding process that combines the PLA structure with the AW causes the polymer to locally melt and infiltrate into the bioceramic structure (Fig 3), providing mechanical adhesion through physical interlocking of the materials. Throughout the in vitro testing no delamination of the PLA from the AW structures was observed, as would be expected on the basis of the slow dissolution rates of these two materials.

4.2 Cellular Assays and Osseointegration

The in vitro assays indicated that, when compared to the PLA alone, the AW material alone best supported proliferation and osteogenic differentiation of the BMSCs. The AW/PLA structure initially showed the same proliferative potential as PLA, but after 48 hours in vitro was similar to the AW. Indications of osteogenic differentiation potential increased from PLA to PLA/AW to AW. This correlates with the known biological responses of both the PLA and AW materials (Hutmacher, 2007; Narayanan, 2016; Dyson, 2007; Lee, 2015).

The in vivo experiments broadly confirmed the in vitro results. The AW material showed excellent osseointegration with the formation of new bone, and vascularisation of the porous AW structure, both for the AW alone and when combined with the PLA. In the absence of AW, the PLA structure was well tolerated however was not osteogenic. Interestingly, the AW/PLA structures showed the largest amount of the newly formed bone in vivo, and the results indicated that the AW and PLA structures could have acted, to some extent, synergistically: the presence of the osteoinductive AW structure appears to have stimulated significant bone growth in the larger pores of the adjacent PLA structure. The exact mechanisms for this are difficult to define: the AW and PLA degradation products might play an important role in tuning the local inflammatory reaction and stimulating osteogenic differentiation of progenitor cells (Williams, 1992; Middleton and Tipton, 2000).

A key concern with layered composite structures is delamination, and no delamination was observed in any of the composite structures, although no loading was applied. In fact the

degree of osseointegration of the composite structure in Figure 6 (c) indicates delamination is unlikely as the structure is effectively bound together by the new bone which has grown into and around the structure. Clearly the structure is only held together by new bone once that bone has formed, and so for immediate stability the bond between the materials needs to have an appropriate inherent strength. With materials which resorbed quicker or did not have the same degree of osseointegration it is considered that the risk of delamination would be much higher.

4.3 Implications for Bone Implant Design

The results offer two key observations for bone implant design based on macro-scale composite structures. Firstly, that it is possible through biocomposites fabricated at a macro-scale to develop implants which provide a match to both cortical and cancellous bone properties. Secondly that to avoid delamination in such structures an appropriate choice of materials and structures can both avoid immediate resorption and promote osseointegration. The mechanical properties of the two phases of the composite are such that the composites could be exploited for implants to treat defects which were of a size which required mechanical support. Clearly an appropriate fixation scheme would be required, but if properly fixed the implants could be immediately load bearing. To improve the composite structures, particularly for larger implants it would be preferable to further enhance the osseoinductivity of the PLA structure. This could be achieved through making the structure from a micro-scale composite of PLA and a bioceramic (nano- or micro- HA, for instance (Tayton et al; 2014), or AW) or through surface functionalisation (with collagen or gelatin for example; Haaparanta et al., 2014). PLA based materials have also been shown to offer utility for drug release (Saini et al., 2016), and so further enhancement of bioactivity could be achieved through incorporating specific molecules into the polymer, with the proviso that any effects on the mechanical properties would have to be carefully monitored.

5. Conclusions

A novel AW/PLA composite structure, which matches cortical and cancellous bone properties over millimetre length scales has been produced. In vitro tests on the composite structure indicated proliferative and osseoinductive properties in between those of AW and PLA alone, but in vivo the combination of the AW and PLA structures supported significant new bone growth. The use of materials which are initially effectively bonded, which do not resorb over short timescales, and which promote significant bone ingrowth is considered an effective strategy to minimise delamination of layer composites in vivo.

6. Acknowledgements

The work presented in this paper has been carried out as part of the EC Framework VII RESTORATION project (Award CP-TP 280575-2), the Arthritis Research UK Tissue Engineering Centre (Award 19429), and the EPSRC Centre for Innovative Manufacture in Medical Devices (Award EP/K029592/1). PhD studentship support from the EPSRC (Rodrigues, Toumpaniari) and the Saudi Arabian Government (Alharbi) is also gratefully acknowledged.

7. References

Allen, M., Millett, P., Dawes, E. and Rushton, N. (1994). Lactate dehydrogenase activity as a rapid and sensitive test for the quantification of cell numbers in vitro. *Clinical Materials*, 16, pp 189-194.

Dyson, J.A, Genever, P.G., Dalgarno, K.W. and Wood, D.J. (2007). Development of Custom-Built Bone Scaffolds Using Mesenchymal Stem Cells and Apatite-Wollastonite Glass-Ceramics. *Tissue Engineering*, 13, pp 2891-2901, doi: 10.1089/ten.2007.0124.

Haaparanta, A.M., Järvinen, E., Cengiz, I.F., Ellä, V., Kokkonen, H.T., Kiviranta, I. and Kellomäki, M. (2014). Preparation and characterization of collagen/PLA, chitosan/PLA, and

collagen/chitosan/PLA hybrid scaffolds for cartilage tissue engineering. *Journal of Materials Science: Materials in Medicine*, 25, pp 1129-1136, doi:10.1007/s10856-013-5129-5.

Hutmacher, D.W., Schantz, J.T., Lam, C.X., Tan, K.C. and Lim, T.C. (2007). State of the art and future directions of scaffold-based bone engineering from a biomaterials perspective. *Journal of Tissue Engineering and Regenerative Medicine*. 1, pp 245-60, doi: 10.1002/term.24.

Keaveny, T.M. and Hayes, W.C. (1993). Mechanical properties of cortical and trabecular bone. In *Bone. A treatise, volume VII: bone growth*, CRC Press. pp. 285 - 344.

Kokubo, T. (1991). Bioactive glass ceramics: properties and applications. *Biomaterials*, 12, pp 155-163, doi: 10.1016/0142-9612(91)90194-F.

Lee, J.A., Knight, C.A., Kun, X., Yang, X.B., Wood, D.J., Dalgarno, K.W. and Genever, P.G. (2015). In vivo biocompatibility of custom-fabricated apatite-wollastonite-mesenchymal stromal cell constructs. *Journal of Biomedical Materials Research Part A*, 10, pp 3188-3200, doi: 10.1002/jbm.a.35448.

Li, B. and Aspden, RM (1997). Mechanical and Materials Properties of the subchondral bone plate from the femoral head of patients with osteoarthritis or osteoporosis. *Annals of the Rheumatic Diseases*, 56, pp 247-254.

Mancuso, E., Alharbi, N., Bretcanu, O.A., Marshall, M., Birch, M.A., McCaskie, A.M., Dalgarno, K.W. (2017). 3D printing of porous load bearing bioceramic scaffolds. *Proceedings of the Institution of Mechanical Engineers, Part H: Journal of Engineering in Medicine*. In Press.

Middleton, J.C. and Tipton A.J. (2000). Synthetic biodegradable polymers as orthopedic devices. *Biomaterials*, 21, pp 2335-2346, doi: 10.1016/S0142-9612(00)00101-0.

Mota, C., Puppi, D., Chiellini, F. and Chiellini, E. (2015). Additive manufacturing techniques for the production of tissue engineering constructs. *Journal of Tissue Engineering and Regenerative Medicine*, 9, pp 174-190, doi: 10.1002/term.1635.

Narayanan, G., Vernekar, V.N., Kuyinua, E.L. and Laurencin, C.T. (2016). Poly (lactic acid)-based biomaterials for orthopaedic regenerative engineering. *Advanced Drug Delivery Reviews*, 107, pp 247–276, doi: 10.1016/j.addr.2016.04.015.

Rezwan, K., Chen, Q.Z., Blaker, J.J. and Boccaccini, A.R. (2006). Biodegradable and bioactive porous polymer/inorganic composite scaffolds for bone tissue engineering. *Biomaterials*, 27, pp 3413-3431, doi: 10.1016/j.biomaterials.2006.01.039.

Rodrigues, N., Benning, M., Ferreira, A.M., Dixon, L., and Dalgarno, K (2016). Manufacture and Characterisation of Porous PLA Scaffolds. *Procedia CIRP*, 49, pp 33-38, doi: 10.1016/j.procir.2015.07.025.

Saini, P., Arora, M. and Ravi Kumar, MNV (2016). Poly(lactic acid) blends in biomedical applications. Advanced Drug Delivery Reviews, 107, pp 47-59, 10.1016/j.addr.2016.06.014.

Tayton, E., Purcell, M., Aarvold, A., Smith, J.O., Briscoe, A., Kanczler, J.M., Shakesheff, K.M., Howdle, S.M., Dunlop, D.G., and Oreffo, R.O.C. (2014). A comparison of polymer and polymer–hydroxyapatite composite tissue engineered scaffolds for use inbone regeneration. An in vitro and in vivo study. Journal of Biomedical Materials Research Part A, 102, pp 2613–2624, doi: 10.1002/jbm.a.34926.

Tour, G., Wendel, M. and Tcacencu, I (2014). Bone marrow stromal cells enhance the osteogenic properties of hydroxyapatite scaffolds by modulating the foreign body reaction. *Journal of Tissue Engineering and Regenerative Medicine*, 8, pp 841-849, doi: 10.1002/term.1574.

Wang, X., Xu, S., Zhou, S., Xu, W., Leary, M., Choong, P., Qian, M., Brandt, M. and Xie, Y.M. (2016). Topological design and additive manufacturing of porous metals for bone scaffolds and orthopaedic implants: A review. *Biomaterials*, 83, pp127-141, doi: 10.1016/j.biomaterials.2016.01.012.

Williams D.F. (1992). Mechanisms of biodegradation of implantable polymers. *Clinical Materials*, 10, pp 9-12, doi: 10.1016/0267-6605(92)90078-8.

Xiao, K., Dalgarno, K.W., Wood, D.J., Goodridge, R.D., & Ohtsuki, C. (2008). Indirect selective laser sintering of apatite-wollastonite glass-ceramic. *Proceedings of the Institution*

of Mechanical Engineers, Part H: Journal of Engineering in Medicine, 222, pp 1107-1114, doi: 10.1243/09544119JEIM41